INDIAN JOURNAL OF SCIENCE AND TECHNOLOGY

ORIGINAL RESEARCH

Controlled Synthesis of Graphitic Carbon Nitride (g-C3N4) For Photocatalytic Degradation of Dyes

Bayazid Bustami[1], Parvej Rahman Alif[2], MD. Zahid Hasan Suman[3], Alam, S. M. Nur[4], Md Mahfuzur Rahman[5]*

1 M.Sc. Eng. Student, Department of Industrial and Production Engineering, Jashore University of Science and Technology, Jashore-7408, Bangladesh
2 B.Sc. Eng. Student, Department of Industrial and Production Engineering, Jashore University of Science and Technology, Jashore-7408, Bangladesh
3 M.Sc. Student, Department of Mathematics, Jashore University of Science and Technology, Jashore-7408, Bangladesh
4 Professor, Department of Chemical Engineering, Jashore University of Science and Technology, Jashore-7408, Bangladesh
5 Assistant Professor, Department of Industrial and Production Engineering, Jashore University of Science and Technology, Jashore-7408, Bangladesh, Tel.: +880 1794-061876

OPEN ACCESS

Received: 24/12/2024

Accepted: 25/02/2025

Published: 08/04/2025

Citation: Bustami B, Alif PR, Suman MDZH, Nur ASM, Rahman MM (2025) Controlled Synthesis of Graphitic Carbon Nitride (g-C3N4) For Photocatalytic Degradation of Dyes. Indian Journal of Science and Technology 18(12): 983-992. https://doi.org/ 10.17485/IJST/v18i12.4093

* **Corresponding author**.

Tel: +880 1794-061876
mrahman.ipe@just.edu.bd

Funding: None

Competing Interests: None

Copyright: © 2025 Bustami et al. This is an open access article distributed under the terms of the Creative Commons Attribution License, which permits unrestricted use, distribution, and reproduction in any medium, provided the original author and source are credited.

Published By Indian Society for Education and Environment (iSee)

ISSN
Print: 0974-6846
Electronic: 0974-5645

Abstract

Objectives: This study aims to synthesize porous g-C_3N_4 nanosheet (PGCN) with enhanced photodegradation properties. As-synthesized photocatalysts were used to degrade organic textile dyes (Rhodamine B) under UV-visible light irradiation. **Method:** Herein, a hybrid approach combining one-step synthesis and thermal exfoliation was used to fabricate exfoliated-PGCN (E-PGCN), where NH_4Cl and melamine were used as raw materials. Robust characterization methods such as SEM (Scanning Electron Microscope), BET (Brunauer-Emmett-Teller), etc. were used to validate the structure and morphology of the as-fabricated photocatalysts. **Findings:** The experimental results revealed that the photocatalytic activity of BGCN, PGCN, and E-PGCN are 59.26%, 71.5%, and 92% respectively. The thermal exfoliation of PGCN (E-PGCN) improved surface area leading to enhanced degradation efficiency of PGCN from 71.5% to 92%, which is even 1.55, and 1.28 times higher than that of BGCN as well as PGCN respectively. **Novelty:** In this study, a tailored, facile, and cost-effective method combining one-step synthesis and thermal exfoliation technique was used to achieve high-yielding porous g-C_3N_4 nanosheets with high stability for enhanced photocatalytic performance. Additionally, the photocatalytic mechanism of E-PGCN for the degradation of Rhodamine B (RhB) has also been proposed.

Keywords: Graphitic Carbon Nitride Nanosheet; Photocatalytic Degradation; Organic Pollutant; Wastewater; Rhodamine B Graphical Abstract

Graphical Abstract

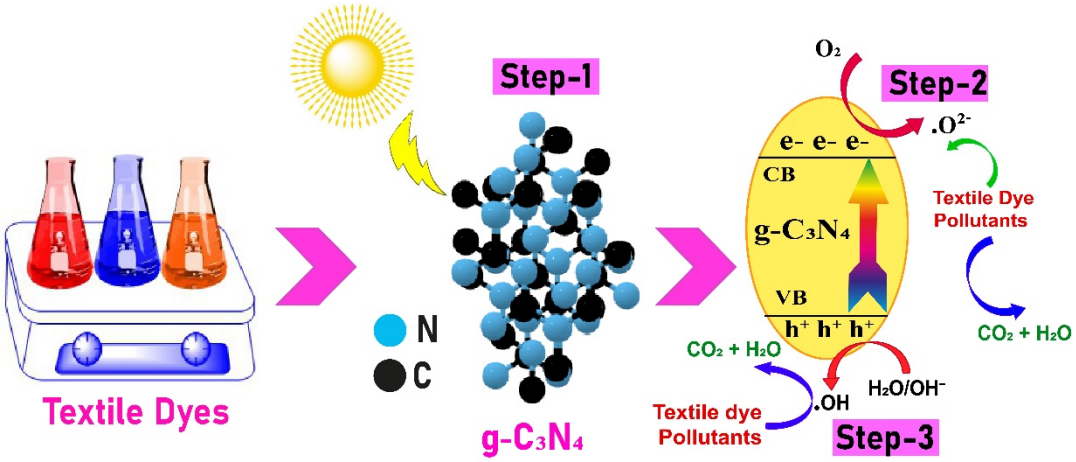

1 Introduction

Human survival depends on the supply of clean water, yet organic pollutants in water are steadily increasing, making it harder to find pure water. Currently, two billion people are drinking contaminated water[1] . The primary sources of water pollution are industrial chemicals, textile dyes, pesticides, herbicides, and byproducts; even in very small amounts, these substances can seriously harm human health[2] . The textile industry is one of the most important to humanity, given that clothing is a fundamental human need. However, the textile sector generates massive amounts of wastewater because finished textile products require 50–100 L of water per kg[3]. E^{v}e^{r}y year, this industry releases between 10% and 15% of the different dyes without the proper physiochemical treatment[3].The textile effluents include a variety of chemicals such as dyes, heavy metals, ammonia (NH_3), sulfide (S^{2-}), lead (Pb), caustic soda (NaOH), Glauber salt (Na_2SO_4), oil, and grease[4] . These released effluents are very harmful to human health and aquatic life biodiversity and are identified as a reason for neurological disorders, anemia, and even cancer[5]. Rhodamine B, the selected contaminant, is a weakly basic nitrogenous molecule that dissociates from a colorful cation which is highly stable and non-biodegradable. It hinders sunlight penetration through water, decreases the rate of photosynthesis in water bodies, raises biological oxygen demands (BOD), and, thereby, destroys the ecosystem. According to ecotoxicological studies, the Predicted No Effect Concentration (PNEC) of rhodamine B in an aquatic organism is 14 μg/L[6]. In humans and animals, it is classified as a neurotoxic dye that can lead to infections of the respiratory, gastrointestinal, skin, and eyes[7]. In this regard, numerous strategies have been reported to remove these hazardous dyes, which involve adsorption, biosorption, ultrafiltration, ion exchange, coagulation, and advanced oxidation process (AOP)[8]. Recently, AOP-based photocatalytic wastewater treatment techniques have been extensively employed for environmental remediation because of their benefits, which include high efficiency, low maintenance costs, ease of use, and environmental friendliness[9]. Photocatalysis has evolved as a green and sustainable solution to eliminate harmful pollutants utilizing renewable solar energy. It leads to the complete decomposition of organic pollutants without forming any secondary pollutants. Moreover, photocatalysis technology has the potential to directly utilize pure, economical, and indestructible solar energy[10]. In the past few decades, a significant number of photocatalysts have been recorded. However, the main obstacles that currently hinder the practical applications of these photocatalysts are their wide band gap, poor stability, and low quantum efficiency[11]. Hence, it is crucial to fabricate and refine a novel photocatalyst that exhibits exceptional photocatalytic activity and maintains a high level of stability under UV-visible light illumination.

Recent research has shown that semiconductor-based photocatalysts are a promising choice for the degradation of organic pollutants due to their high catalytic activity, high turnover number, strong oxidizing capacity, and several other desirable properties[12]. Notably, Graphitic carbon nitride (GCN), a visible light active organic polymer semiconductor photocatalyst, has grabbed a lot of attention for the degradation of organic contaminants due to its strong thermal and chemical stability, low cost, non-toxicity, modest bandgap (2.7 eV) and simple preparation method[13]. Despite these great qualities, the photocatalytic activity of GCN is constrained by its quick charge carrier recombination and low visible light absorption. Moreover, GCN's low solar absorption characteristics limit its photocatalytic activity. Therefore, it is imperative to enhance the photocatalytic performance of GCN.

To improve the g-C_3N_4's properties and photoactivity several modification methods of g-C_3N_4 are reported, such as doping, nanostructure design, or formation of heterojunctions with different materials[14,15]. ^{Am}on^{g} these methods, the design

of nanostructured g-C_3N_4 has been deeply probed by researchers. Porous g-C_3N_4 nanosheets have been synthesized using a variety of techniques. One of the simplest techniques is exfoliation technology. The thermal exfoliation process of g–C_3N_4 is a straightforward technique for the synthesis of a catalyst that exhibits excellent porosity and degradation efficiency, making it suitable for many environmental applications. Based on previously published research, several researchers developed thermal exfoliation of g–C_3N_4 with varying precursors and parameters for applications such as dye degradation, NO_x removal, and production of H_2. Recently, S Ganesan et al. synthesized exfoliated g–C_3N_4 to remove RhB from water[16]. Their result revealed that the degradation efficiency for RhB was approximately 95%[16]. Amiri et al. also used the exfoliation method to prepare g–C_3N_4 nanosheets and found that the RhB degradation efficiency is around 93.5%[17].

The one-step synthesis technique was also widely employed by researchers to fabricate g-C_3N_4 nanosheets for many environmental applications. Y Hong et al. also prepared g-C_3N_4 nanosheets by one-step synthesis technique for boosting photocatalytic hydrogen production[18]. Recently, A Xia et al. synthesized PGCN by using the one-step route for efficient production of H_2O_2 through photocatalytic degradation of atrazine[19]. The one-step technique was also employed by Hoang et al. to fabricate PGCN. The findings confirmed that the fabricated catalysts degraded the most common textile dyes such as methylene blue, methyl orange, and rhodamine B dye solutions under UV light illumination. Their fabricated photocatalyst demonstrated 98% RhB removal after 210 min of visible light irradiation[20].

Herein, we reported a tailored, facile, and cost-effective fabrication of E-PGCN by thermal exfoliation of PGCN where PGCN was obtained by thermally treating melamine powder in a one-step process in the presence of NH_4Cl. The pretreatment of melamine powder with NH_4Cl improved the quality and the photocatalytic properties of PGCN. Direct calcination of melamine powder without any pretreatment gave us a less porous structure called BGCN. A robust characterization technique combined with SEM, BET, FTIR and UV-visible absorption spectroscopy has been employed for the comparative analysis of the as-synthesized BGCN, PGCN and E-PGCN. The photocatalytic degradation efficiency of the as-prepared catalysts against the most common textile dye, such as rhodamine B (RhB), under UV light irradiations has been evaluated. Furthermore, we investigated the mechanisms through which the photocatalysts degraded the organic dyes (RhB). To the best of our current understanding, no study fabricated porous g-C_3N_4 nanosheets by the tailored method of one-step synthesis and thermal exfoliation method for the photodegradation of textile dyes. This work facilitates a deeper understanding of the controlled synthesis of GCN with tunable photocatalytic properties.

2 Methodology

2.1 Material and Chemicals

Melamine ($C_3H_6N_6$) powder (Merck KGaA, Germany), and Ammonium chloride (NH_4Cl) (Research-Lab, India) were purchased commercially and used directly without further purification. The Rhodamine B dye (CI 45170) was acquired from LOBA Chemie Ltd. (INDIA) and used without performing any physical or chemical modifications. It has the molecular weight of 479.02 g mol^{-1} and the chemical formula $C_{28}H_{31}ClN_2O_3$ [6]. Figure 1 shows the chemical structure of the dye. All aqueous solutions were prepared with the deionized water (DI) water.

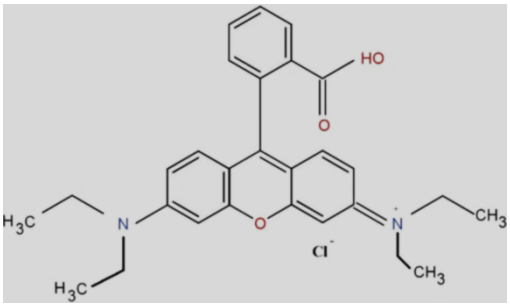

Fig 1. A schematic diagram showing the chemical structure of Rhodamine B[6]

2.2 Catalyst Synthesis

2.2.1. Synthesis of BGCN

The bulk g-C_3N_4 (BGCN) was synthesized by thermal polycondensation of melamine powder under high temperatures. In the standard process, 10 g of melamine was calcinated for 4 h at 550 °C with 5 °C min^{-1} ramping temperature, then by naturally cooling to room temperature. Finally, the obtained sample was bulk g-C_3N_4 (BGCN), which was ground into a fine yellowish powder.

2.2.2. Synthesis of PGCN and E-PGCN

The exfoliated porous g-C_3N_4 nanosheets (E-PGCN) samples were prepared in two steps. At first, melamine powder was thermally treated in the presence of NH_4Cl in a single step to fabricate the porous g-C_3N_4 nanosheet (PGCN) powder. Here, 4.0g of melamine powder and 16g of NH_4Cl were mixed (with a mass ratio of 1:4) and then ground for 15 min. The mixture was then calcinated for 4 h at 550 °C with the ramping temperature of 2 °C min^{-1} and normally cooled to room temperature. The yellow product was collected, cooled, and ground to prepare PGCN powder. In order to produce an exfoliated structure with improved porosity and photocatalytic properties, PGCN was thermally heated in an open alumina crucible at 550 °C for two hours at a rate of 5 °C per minute. The exfoliated structure was dubbed E-PGCN, and this procedure is called thermal exfoliation. Figure 2 depicts the complete synthesis steps of both BGCN and E-PGCN.

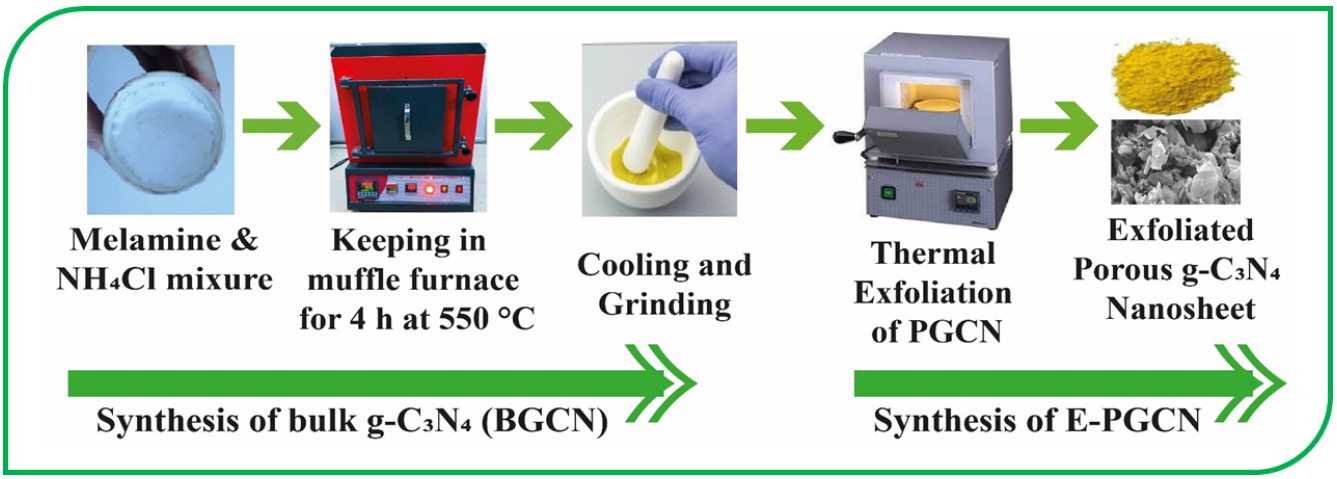

Fig 2. Schematic diagram showing the fabrication process ofBGCN, and E-PGCN

2.3 Catalysts Characterization

The morphologies and structures of the samples were identified by scanning electron microscopy (SEM). The changes in the structures and compositions of the modified materials were further investigated using Fourier transform infrared spectroscopy (FTIR), and Energy Dispersive Spectroscopy (EDS). Brunauer-Emmett-Teller (BET) analysis was conducted to obtain the specific surface area and the pore size distribution. The absorption performance of the catalysts was also observed by employing UV-vis absorbance spectra analysis.

2.4 Photocatalytic Activity of the Prepared Catalysts

Using rhodamine B (RhB) as a model pollutant, the photocatalytic activity of the as-fabricated catalysts in aqueous solution was assessed by exposing them to UV-visible light. Firstly, as prepared RhB solution with the catalysts were stirred for 30 minutes in the dark to minimize the effect of external factors such as light sources etc. After the dark period, the stable mixture was exposed to UV-visible light for photocatalytic reactions. In an experiment, 300 mg of the as-fabricated photocatalyst was added to 50 mL of a 20 ppm RhB solution while being constantly agitated in order to assess the degradation efficiency of BGCN and PGCN for RhB in aqueous solution. The catalyst-containing solution was exposed to visible light while being continuously stirred by magnetic forces. After being exposed to radiation for 165 minutes, 10 milliliters of the suspensions were removed from the reaction system and centrifuged to extract the photocatalyst particles for examination. The residual concentration of the RhB

solution was then determined by analyzing the characteristic absorption peak obtained from the UV-visible spectrometer. The relative concentration (C/C_O) of the RhB solution was calculated at 554 nm (λ_{max} = 554). The final degradation efficiency of RhB could be calculated according to the formula:

$$\text{Efficiency} = \left\{ \frac{C_0 - C}{C_0} \right\} \times 100 \quad (1)$$

where C_O and C are the concentrations of RhB at the beginning of light irradiation and at time t, correspondingly.

3 Results and Discussion

3.1 FT-IR analysis

In order to determine the stability and crystal structure of GCN, FT-IR was used to examine the synthesized photocatalysts. Figure 5a shows the results obtained from FT-IR characterizations of the g-C_3N_4 photocatalysts fabricated at different conditions. A range of wavenumber 700 to 3500 cm^{-1} was used to record FT-IR signal. There aren't any noticeable distinctions between BGCN, PGCN, and E-PGCN in their typical FT-IR spectra. It is obvious that BGCN, PGCN, and E-PGCN possess the same chemical structure. The broad peak between 3500 and 3000 cm^{-1} is associated with the O-H and N-H stretching vibration modes from adsorbed water on the surface. Aromatic C–N heterocyclic units exhibit vibrational absorption in the range of 1200–1600 cm^{-1} [16]. The sharp peak at around 800 cm^{-1} is the characteristic peak of the tri-s-triazine units. The peak intensity at 1680 to 1200 cm^{-1} in the modified GCNs may also be significantly increased by the presence of a lot of ammonia gas. At the same time, it is evident that the modified carbon nitrides (PGCN, and E-PGCN) are significantly increased at the peak of 3500 to 3000 cm^{-1}. This suggests that the PGCN and E-PGCN contain more amino groups when a significant amount of ammonia is present [20].

3.2 Structural Analysis

The structure and morphology of the as-synthesized BGCN and PGCN were determined by field emission scanning electron microscope (FESEM) and energy dispersive spectroscopy (EDS) mapping, and the results are shown in Figure 3. FESEM images of the as-prepared BGCN (Figure 3a) showed the formation of bigger particles in 3D shape. The average length as well as width of the particle are about 4.95 μm and 0.841 μm respectively. A zoomed view of the FESEM images displays some local interspaces among the diverse layers in BGCN. The EDS spectra presented in Figure 3b, confirm that the synthesized BGCN catalyst is mainly composed of C and N, however, it contains some Au particles due to the sputtering of GCN before SEM characterization.

On the other hand, the NH_4Cl-modified g-C_3N_4 (PGCN) has a porous structure as displayed in Figure 3c along with a zoomed view for better understanding. In porous g-C_3N_4 nanosheets, the layers are smaller and 2D in shape with more intermolecular spaces. The average length of the particle is about 2.129 μm. Due to the porous structure, light absorption capability is enhanced thereby increasing the photocatalytic activity of the as-synthesized PGCN photocatalysts. The EDS spectra (Figure 3d) showed that the as-prepared PGCN samples mainly consist of C and N. As the PGCN sample was fabricated by the pretreatment melamine with NH_4Cl, it contains Cl particles. The other particles including Nb and Rb were found due to Au sputtering before SEM characterization.

3.3 Surface Area and Porosity Analysis

Brunauer-Emmett-Teller (BET) analysis of the as-synthesized g-C_3N_4 samples was conducted and the results are summarized in Table 1. N_2 adsorption-desorption isotherm and the pore size distribution of the as prepared photocatalysts' are displayed in Figure 4. With pore sizes ranging from 2 to 50 nm, the observed pattern specifically emphasizes the mesoporous nature of the as-synthesized E-PGCN.

BET surface areas for the BGCN and E-PGCN were 21.32 and 47.93 m^2/g respectively. By the formation of the pores and nanostructures, the BET surface area was significantly enhanced to 47.93 m^2/g for E-PGCN. Similarly, the pore volume of BGCN and E-PGCN were 0.1067 and 0.1264 cm^3/g respectively. Large BET surface area and pore volume are desirable because they increase the photocatalytic degradation activity of the photocatalyst. This is explained by the fact that more pollutants can be adsorbed due to the large surface area. As a result, the photocatalytic degradation performance of the E-PGCN sample will be superior.

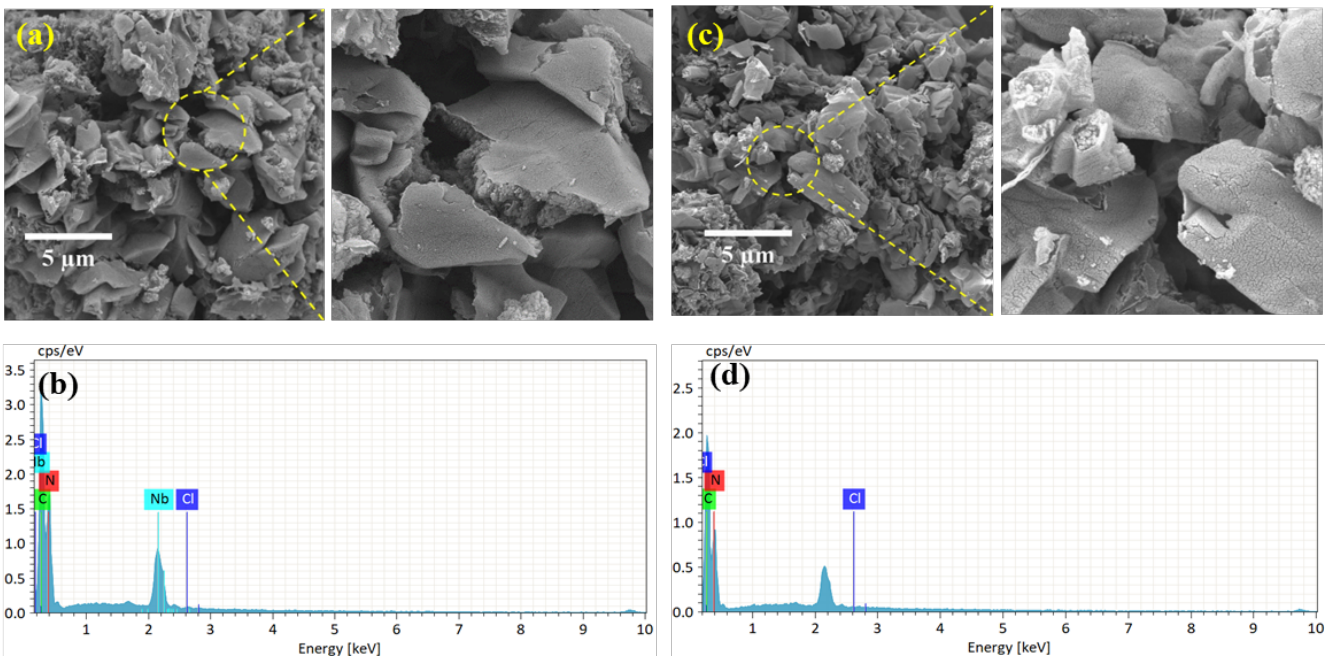

Fig 3. Structural and morphological characterization. (a) FESEM images of BGCN, (b) EDS spectra of BGCN, (c) FESEM images of PGCNs, (d) corresponding EDS spectra

Table 1. ET surface areas, total pore volumes, and average pore sizes of the fabricated catalysts

Sample	BET surface area (m^2/g)	Total pore volume (cm^3/g)	Average pore size (nm)
BGCN	21.32	0.1067	20.029
E-PGCN	47.93	0.1264	10.552

3.4 Optical Properties

From the UV–vis absorbance spectra of BGCN, PGCN, and E-PGCN throughout a wavelength range of 400–650 nm, shown in Figure 5b, display the absorbance behavior of the samples. From the UV-vis absorption spectra, it is observed that the principal absorption peak is centered at 554 nm, suggesting a comparable photoluminescent response. Thus, as prepared samples contain photoactive elements or structure that absorb light in this wavelength. The green line, or BGCN, in Figure 5 exhibits the highest peak intensity, just above 0.4 absorbance units (a.u.), suggesting that a sizable amount of dye is still present. Accordingly, BGCN's high absorption intensity indicates a higher charge carrier recombination rate leading to the lowest dye degradation efficiency. On the other hand, E-PGCN (blue line) has the weakest peak intensity, just above 0.2 a.u., indicating that GCN's photocatalytic capabilities are improved when it is treated with NH_4Cl, which effectively suppresses charge carrier recombination.

3.5 Photocatalytic Performance Testing

As synthesized BGCN, PGCN, and E-PGCN were used photocatalysts to study the performance for the degradation of Rhodamine B (RhB) both in dark and light conditions. In order to evaluate each catalyst's degradation performance, the process was first carried out in the dark for 30 minutes. After that, light irradiation for 165 minutes was applied to promote photocatalytic activity. Degradation efficiency was calculated using equation (1) at the wavelength of peak position about 554 nm.

From Figure 5(c)-(d), it can be observed clearly that E-PGCN demonstrated superior degradation efficiency, followed by BGCN and PGCN. Specifically, after 165 minutes of visible light exposure, RhB degradation rates were recorded as 59.26% for BGCN, 71.5% for PGCN, and 92% for E-PGCN. The enhanced activity of E-PGCN is attributed to its higher surface area and efficient charge separation, facilitating the generation of active radicals that effectively break down RhB molecules[16]. In comparison, E-PGCN exhibited a degradation rate of 1.55 and 1.28 times that of BGCN and PGCN respectively, highlighting its effectiveness as a photocatalyst for the removal of organic pollutants. This study highlights how thermally exfoliated PGCN can enhance environmental remediation procedures and provide a sustainable, effective wastewater treatment solution.

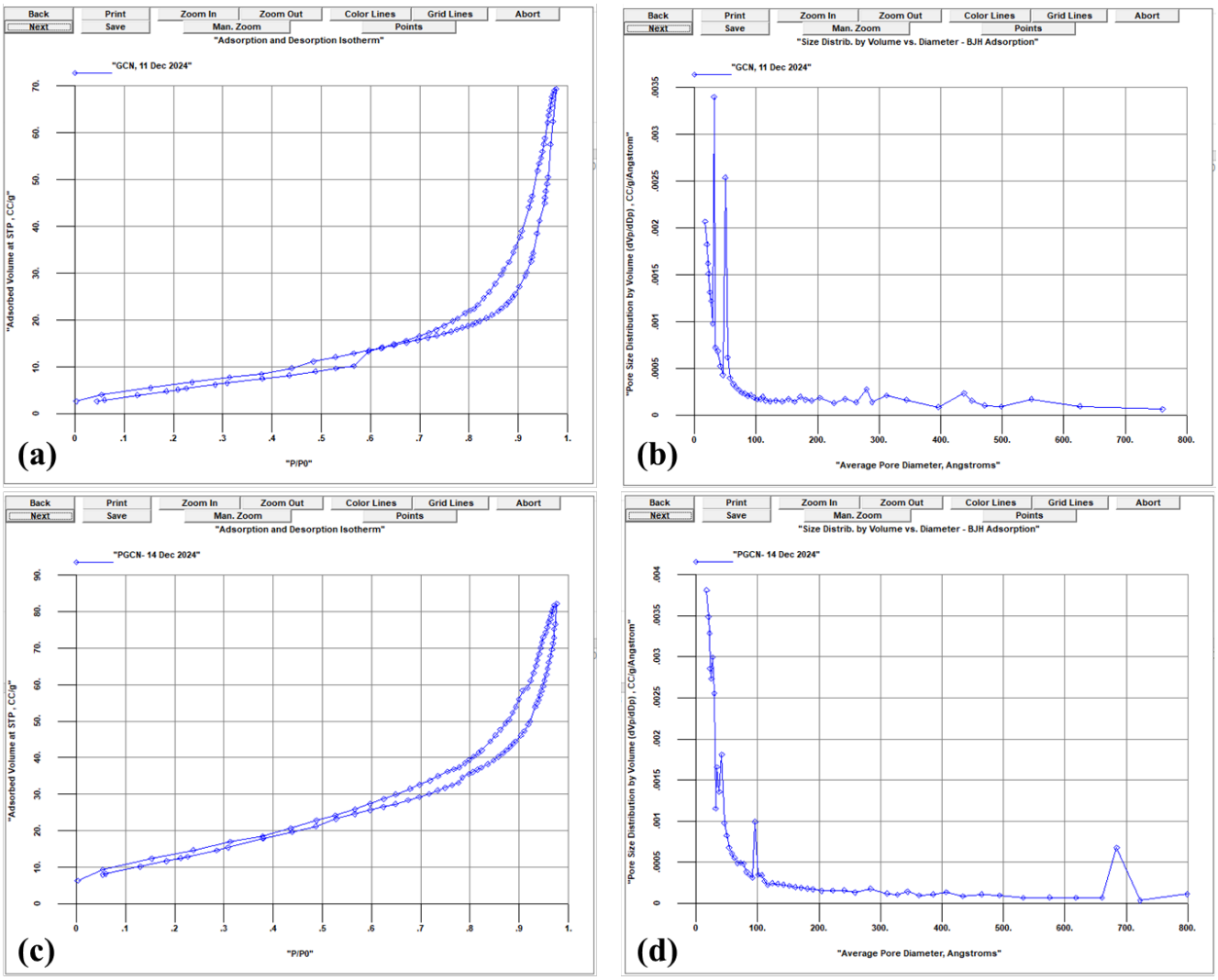

Fig 4. BET analysis: (a)N_2 adsorption/desorption isotherms of BGCN, (b) corresponding pore size distribution of BGCN, and (c) N_2 adsorption/desorption isotherms of E-PGCN and (d) corresponding pore size distribution curves of E-PGCN

3.6 Catalytic mechanism

It is commonly known that when photons with energies more than or equal to the band gap energy (Eg) are absorbed by a semiconductor particle, the photocatalytic process begins. These photons are absorbed, producing electron-hole pairs in the bulk that split into free photoelectrons in the CB and holes in the VB. A hole (h^+), which has a +ve charge and works as a charge carrier, is formed in the valence band (VB) when an electron (e^-) from the VB is transferred to the conduction band (CB). Under visible light, g-C_3N_4 produces electron-hole pairs when electrons are stimulated from the valence band (VB) to the conduction band (CB). The separated electrons (e^-) and holes (h^+) go to the surface of the material and start redox reactions. The VB holes create hydroxyl radicals (• OH), while the CB electrons create superoxide radicals (• O_2^-). These reactive species use a photocatalytic mechanism to break down contaminants like RhB. The entire mechanism of photocatalytic degradation of organic pollutants (RhB) under visible light on g-C_3N_4 is shown in Figure 6 and detailed in Equations (2) – (5).

$$g-C3N4 + h\nu \rightarrow e- + h+ \tag{2}$$

$$O^2 + e^- \rightarrow \cdot O_2^- \tag{3}$$

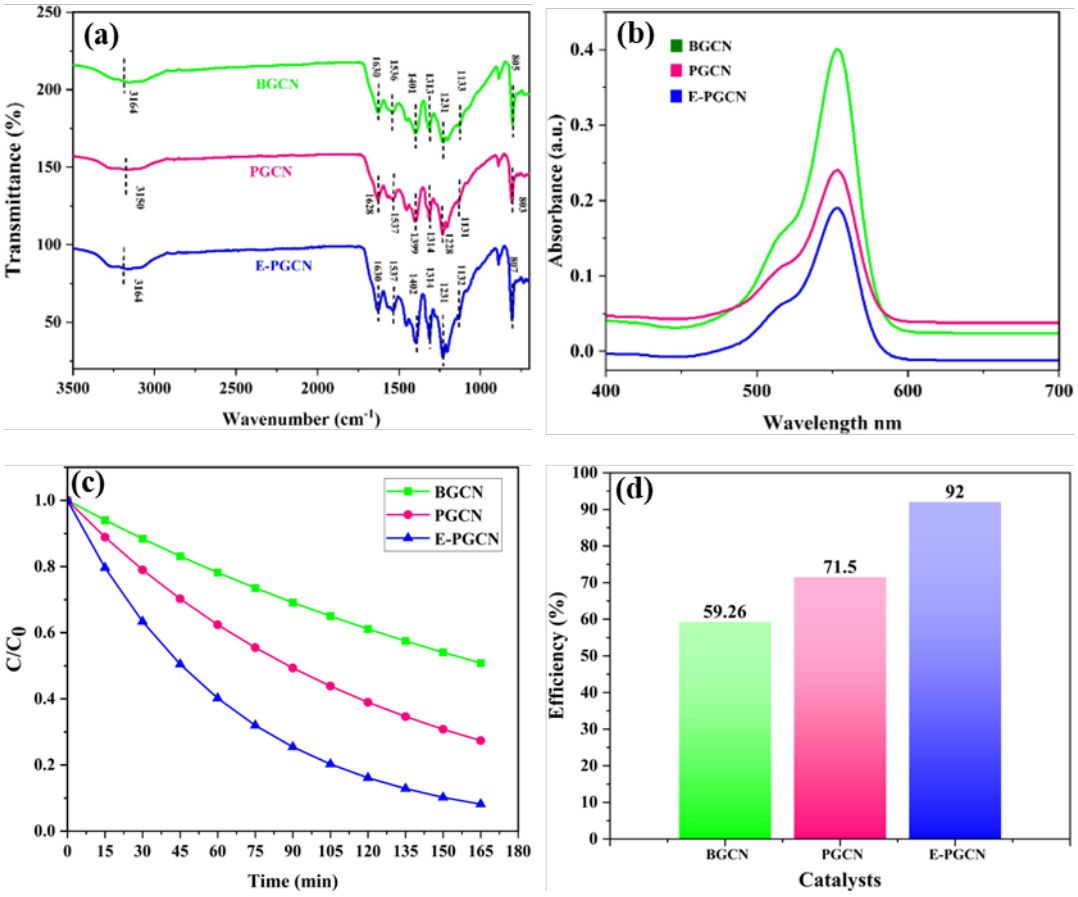

Fig 5. (a) UV–vis spectra of BGCN, PGCN, and E-PGCN, (b) FTIR spectrum of the BGCN, PGCN, and E-PGCN captured in pure forms, (c) Time profiles of the degradation of RhB, and (d) photocatalytic efficiency of different catalysts

$$H_2O + h^+ \rightarrow \cdot OH + H^+ \tag{4}$$

$$\cdot O_2^- / \cdot OH + \text{ Pollutants (RhB)} \rightarrow \text{ Degradation Products } (CO_2 + H_2O) \tag{5}$$

The ideal conditions for the degradation of a particular organic pollutant may vary depending on the type of photocatalyst. As a result, it is challenging to precisely compare how efficient their performances are. The indirect comparison of the photocatalytic performance of g-C_3N_4 photocatalysts reported by different researchers is shown in Table 2. The method reported here synthesized catalysts without the application of any strong oxidizing agent or radical scavenger and also has a higher degradation efficiency than catalysts 2, and 5, and a lower degradation efficiency than catalysts 3, 4, 6, and 7 (Table 2). However, the degradation time of our catalyst to decompose RhB was longer than that of catalysts 1-5 and shorter than that of catalysts 6 and 7. The synthesized g-C_3N_4 obtained in this study demonstrated satisfactory results in both photocatalytic performance, in terms of short irradiation time, and high dye concentration when compared to the literature.

4 Conclusion

The porous g-C_3N_4 nanosheet (PGCN) was successfully fabricated by the one-step thermal treatment of melamine in the presence of NH_4Cl and the porosity was further improved by thermally exfoliating the pre-fabricated PGCN photocatalyst at 550 °C. It was observed that NH_4Cl worked as an effective gaseous bubble template with melamine to create porous structures in

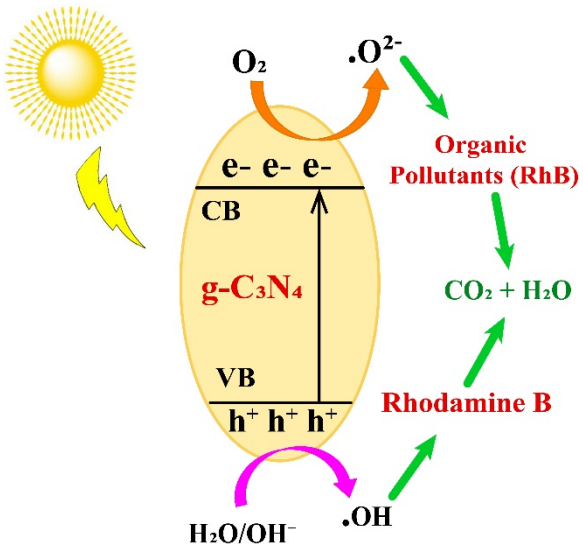

Fig 6. A schematic diagram showing the photocatalytic mechanism of graphitic carbon nitride photocatalyst

Table 2. Comparison of g-C_3N_4 photocatalysts for photocatalytic degradation of organic dyes (RhB)

Catalyst No.	Catalyst	Reaction Conditions	Illumination time	Efficiency	Ref.
01	g-C_3N_4 Nanosheet	10 mg/L RhB solution, visible light	60 min	93.5%	(17)
02	Nano exfoliated	20 mg/L RhB solution, solar light	60 min	78%	(21)
03	g-C_3N_4	10 mg/L RhB solution, visible light	90 min	97.5%	(22)
04	S-doped g-C_3N_4 nanosheets	10 mg/L RhB solution, visible light	60 min	92.64%	(23)
05	g-C_3N_4	20 mg/L Tetracycline solution, visible light	40 min	77%	(24)
06	Porous g-C_3N_4 nanofilm	20 mg/L RhB solution, UV light	210 min	98%	(20)
07	g-C_3N_4 Nanosheet	0.05 mM RhB, direct sunlight	320 min	95%	(25)
08	Porous g-C_3N_4 Nanosheet	20 mg/L RhB solution, UV-visible light	165 min	92%	This work

g-C_3N_4 nanosheets. The modifications also found that exfoliated PGCN (E-PGCN) substantially upgraded the photocatalytic degradation efficiency of PGCN from 71.5 % to 92%. The photodegradation efficiency of E-PGCN is 1.55, and 1.28 times higher than that of BGCN, and PGCN respectively. This considerable enhancement in the photocatalytic performance of E-PGCN is attributed to the novel hybrid synthesis technique that improved the morphology of porous g-C_3N_4 nanosheet. However, there are still some restrictions that call for more research. Although RhB was employed as a model pollutant, the wide variety of organic contaminants found in actual wastewater is not entirely represented. Additionally, the degradation time of synthesized catalysts is longer than that of several other catalysts that have been previously reported. Reducing this degradation period through co-catalyst incorporation or synthesis parameter optimization should be the main goal of future research. For industrial applications, assessing the synthesis process's, scalability, and economic viability is also essential. Furthermore, there are still unanswered problems, such as whether the synthesis method could be modified to improve photocatalytic degradation in the presence of natural sunlight, and how E-PGCN functions in actual wastewater specimens with intricate pollutant and ion mixtures.

References

1) Saher R, Hanif MA, Mansha A, Javed H, Zahid M, Nadeem N. Sunlight-driven photocatalytic degradation of rhodamine B dye by Ag/FeWO 4/gC 3 N 4 composites. *International Journal of Environmental Science and Technology*. 2021;18:927–965. doi:10.1007/s13762-020-02888-6.

2) Karri RR, Ravindran G, Dehghani MH. Wastewater-sources, toxicity, and their consequences to human health. *Soft computing techniques in solid waste and wastewater management*. 2021;p. 3–33. doi:10.1016/B978-0-12-824463-0.00001-X:.
3) Sarwar B, Khan AU, Aslam M, Bokhari A, Mubashir M, Alothman AA. Comparative study of ZIF-8-materials for removal of hazardous compounds using physio-chemical remediation techniques. *Environ Res*. 2023;220:115168–115168. doi:10.1016/j.envres.2022.115168.
4) Khan MD, Singh A, Khan MZ, Tabraiz S, Sheikh J. Current perspectives, recent advancements, and efficiencies of various dye-containing wastewater treatment technologies. *Journal of Water Process Engineering*. 2023;53:103579–103579. doi:10.1016/j.jwpe.2023.103579.
5) Das B, Devi M, Deb S, Dhar SS. Boosting photocatalytic property of graphitic carbon nitride with metal complex fabrication for efficient degradation of organic pollutants. *Chemosphere*. 2023;323:138230–138230. doi:10.1016/j.chemosphere.2023.138230.
6) Sharma J, Sharma S, Bhatt U, Soni V. Toxic effects of Rhodamine B on antioxidant system and photosynthesis of Hydrilla verticillata. *Journal of Hazardous Materials Letters*. 2022;3:100069–100069. doi:10.1016/j.hazl.2022.100069.
7) Imam SS, Babamale HF. A Short Review on the Removal of Rhodamine B Dye Using Agricultural Waste-Based Adsorbents. *Asian Journal of Chemical Sciences*. 2020;7(1):25–37. doi:10.9734/ajocs/2020/v7i119013.
8) Khan WU, Ahmed S, Dhoble Y, Madhav S. A critical review of hazardous waste generation from textile industries and associated ecological impacts. *Journal of the Indian Chemical Society*. 2023;100(1):100829–100829. doi:10.1016/j.jics.2022.100829.
9) Sinha TK. Nanostructured Materials for Visible Light Photocatalysis. AK N, NK S, editors;Elsevier. 2022. Available from: https://doi.org/10.1016/B978-0-12-823018-3.00012-9.
10) Chen D, Cheng Y, Zhou N, Chen P, Wang Y, Li K. Photocatalytic degradation of organic pollutants using TiO2-based photocatalysts: A review. *Journal of Cleaner Production*. 2020;268:121725–121725. doi:10.1016/j.jclepro.2020.121725.
11) Dang Y, Hu Q, He P, Ren T. Tailoring the ratio of ammonium chloride and graphitic carbon nitride for high photocatalytic activity. *Journal of Molecular Structure*. 2020;1209:127961–127961. doi:10.1016/j.molstruc.2020.127961.
12) Duoerkun G, Zhang Y, Shi Z, Shen X, Cao W, Liu T. Construction of n-TiO2/p-Ag2O Junction on Carbon Fiber Cloth with Vis-NIR Photoresponse as a Filter-Membrane-Shaped Photocatalyst. *Advanced Fiber Materials*. 2020;2(1):13–23. doi:10.1007/s42765-019-00025-8.
13) Singh R, Chauhan M, Garg P, Sharma B, Attri P, Sharma RK. A critical review on visible light active graphitic carbon nitride (g-CN) based photocatalyst for environment remediation application: A sustainable approach. *Journal of Cleaner Production*. 2023. doi:10.1016/j.jclepro.2023.138855.
14) Sharma R, Almáši M, Nehra SP, Rao VS, Panchal P, Paul DR. Photocatalytic hydrogen production using graphitic carbon nitride (GCN): A precise review. *Renewable and Sustainable Energy Reviews*. 2022;168:112776–112776. doi:10.1016/j.rser.2022.112776.
15) Younes H, Kuang X, Lou D, Devries B, Rahman MM, Hong H. Magnetic-field-assisted DLP stereolithography for controlled production of highly aligned 3D printed polymer-Fe3O4@graphene nanocomposites. *Materials Research Bulletin*. 2022;154:111938–111938. doi:10.1016/j.materresbull.2022.111938.
16) Ganesan S, Kokulnathan T, Sumathi S, Palaniappan A. Efficient photocatalytic degradation of textile dye pollutants using thermally exfoliated graphitic carbon nitride (TE-g-C3N4). *Scientific Reports*. 2024;14(1):2284–2284. doi:10.1038/s41598-024-52688-y.
17) Amiri S, Yazdani F, Mortaheb H. Exfoliated graphitic carbon nitride nanosheets for visible light photocatalytic degradation of Rhodamine B - Investigation on exfoliation method. *Materials Chemistry and Physics*. 2023;301:127623–127623. doi:10.1016/j.matchemphys.2023.127623.
18) Hong Y, Liu E, Shi J, Lin X, Sheng L, Zhang M. A direct one-step synthesis of ultrathin g-C3N4 nanosheets from thiourea for boosting solar photocatalytic H2 evolution. *International Journal of Hydrogen Energy*. 2019;44(14):7194–204. doi:10.1016/j.ijhydene.2019.01.274.
19) Xia A, Tian H, Huang D, Fang Y, Ye L, Huang Y. Fabricated layered g-C3N4 nanosheets for high efficiency photocatalytic degradation of atrazine:Insight into terminal-NHx in-situ activation of H2O2. *Journal of Environmental Chemical Engineering*. 2024;12(3):112882–112882. doi:10.1016/j.jece.2024.112882.
20) Hoang LA, Le ND, Nguyen TD, Lee T. One-Step Synthesis of g-C3N4 Nanosheets with Enhanced Photocatalytic Performance for Organic Pollutants Degradation Under Visible Light Irradiation. *Topics in Catalysis*. 2023;66(1):194–204. doi:10.1007/s11244-022-01734-y.
21) Pattnaik SP, Behera A, Martha S, Acharya R, Parida K. Facile synthesis of exfoliated graphitic carbon nitride for photocatalytic degradation of ciprofloxacin under solar irradiation. *Journal of Materials Science*. 2019;54(7):5726–5768. doi:10.1007/s10853-018-03266-x.
22) Kadam AN, Kim H, Lee SW. Low-temperature in situ fabrication of porous S-doped g-C3N4 nanosheets using gaseous-bubble template for enhanced visible-light photocatalysis. *Ceramics International*. 2020;46(18):28481–28490. doi:10.1016/j.ceramint.2020.08.005.
23) Narkbuakaew T, Sujaridworakun P. Synthesis of Tri-S-Triazine Based g-C3N4 Photocatalyst for Cationic Rhodamine B Degradation under Visible Light. *Topics in Catalysis*. 2020;63(11):1086–96. doi:10.1007/s11244-020-01375-z.
24) Wang S, Hou M, Fu H, Ruan Z, Sun T, Zhu Y. Synthesis of ultrathin porous g-C3N4 nanofilm via template-free method for photocatalytic degradation of tetracycline. *Journal of Alloys and Compounds*. 2023;939:168738–168738. doi:10.1016/j.jallcom.2023.168738.
25) Yadav AA, Kang SW, Hunge YM. Photocatalytic degradation of Rhodamine B using graphitic carbon nitride photocatalyst. *Journal of Materials Science: Materials in Electronics*. 2021;32(11):15577–85. doi:10.1007/s10854-021-06106-y.